Electronic Supplementary Material (ESI) for Materials Advances.
This journal is © The Royal Society of Chemistry 2024

Protein nanofibrils/polysaccharides aerogel beads as porous functional bio-adsorbent for water treatment

Mandana Dilamian, [a] Majid Montazer, [b] Hossein Yousefi, [c,d] Daniel E. Otzen,[e] Dina Morshedi, [a]*

[a] Bioprocess Engineering Department, Institute of Industrial and Environmental Biotechnology, National Institute of Genetic Engineering and Biotechnology (NIGEB), P.O. Box 14965/161, Tehran, Iran.

[b] Department of Textile Engineering, Amirkabir University of Technology (Tehran Polytechnic), 15875-4413 Tehran, Iran.

[c] Laboratory of Renewable Nanomaterials, Department of Wood Engineering and Technology, Gorgan University of Agricultural Sciences and Natural Resources, Gorgan, 4913815739, Iran.

[d] Nanonovin Polymer Co., Gorgan University of Agricultural Sciences and Natural Resources, 4913815482 Gorgan, Iran.

[e] Interdisciplinary Nanoscience Centre (iNANO), Department of Molecular Biology and Genetics, Aarhus University, 8000 Aarhus C, Denmark.

List of abbreviation

βLG	β-lactoglobulin
CA	Citric Acid
CNFs	Cellulose nanofibers
CR	Congo red
Cs	Chitosan
CPCs	CNFs/Cs/PNFs aerogel beads
PNFs	Protein nanofibrils
PNFs-C	Cross-linked protein fibrils
ThT	thioflavin T

Assessment of protein nanofibrils formation

thioflavin T (ThT) fluorescence experiments were applied to explore the formation of the protein nanofibrils for purified (PNFs) and cross-linked protein fibrils (PNF-C) [1,2]. The sharp fluorescence intensity of ThT for all samples suggested that β-lactoglobulin (βLG) was actively involved in the fibril formation (Fig. S1A). In another test, equal amounts of purified PNFs and cross-linked PNFs solutions were drop-cast into a silicon mold. The solutions contained two different concentrations of citric acid (CA) (1 and 1.5 wt. %). The PNFs solution was evenly distributed on the substrate and then dried in an oven at 65℃ for 10 h. The test result interestingly revealed (Fig. S1B-1) the brittleness of the purified PNFs film and its failure to form a uniform film, demonstrating the low mechanical property of PNFs [3]. In contrast, the protein solutions incorporated with CA resulted in free-standing, homogeneous, flexible films (Fig. S1B-2). These valuable findings demonstrated the efficient integration of CA into the PNFs chains. However, increasing the CA concentration to 1.5 wt. % reduced the flexibility of the films (Fig. S1B-3). Consequently, PNF-C1 was selected as the highly effective cross-linked PNFs solution.

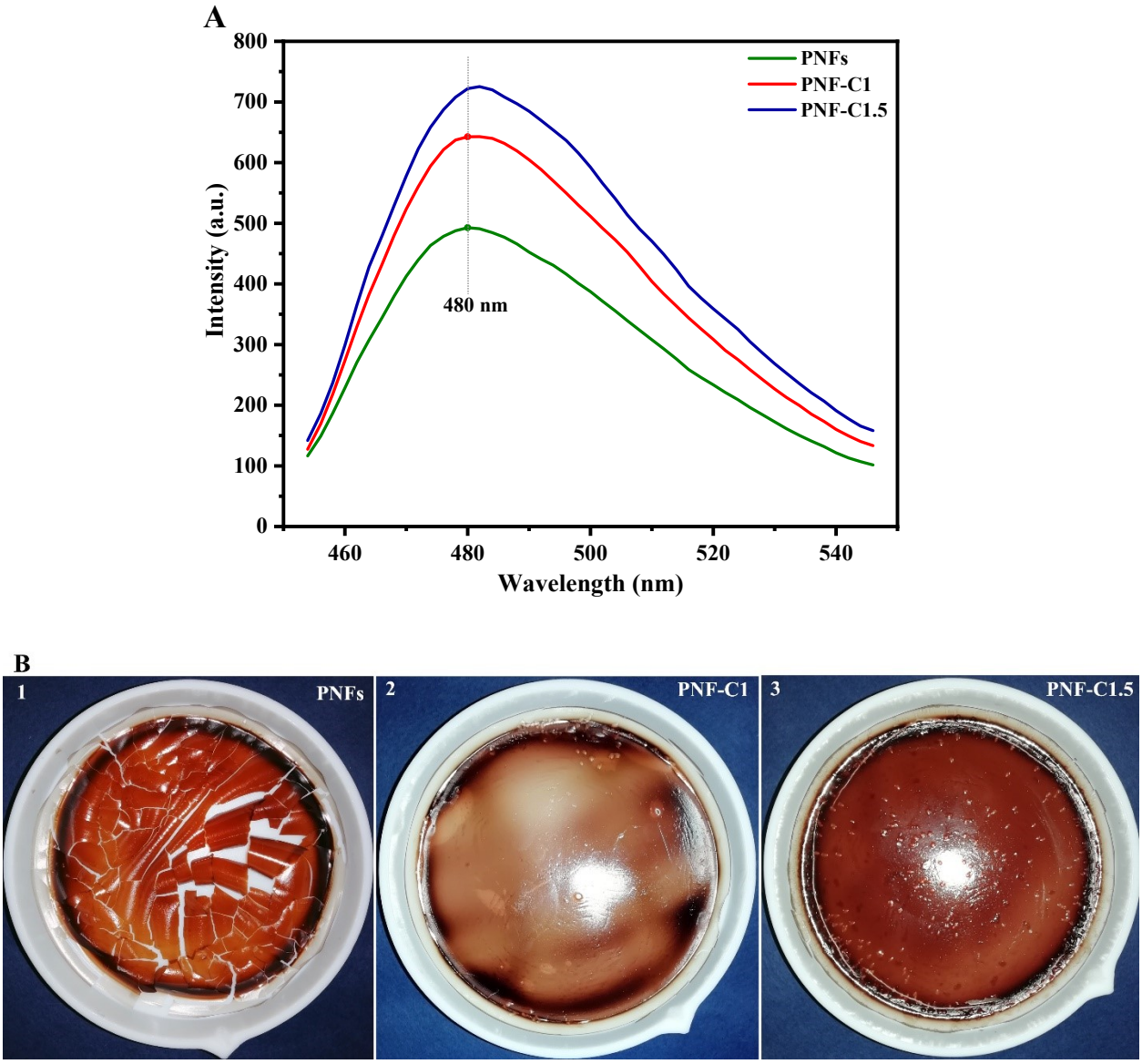

Fig. S1 (A) ThT fluorescence spectra of PNFs in the absence (PNFs, represented by the green line) and presence of CA with different concentrations (PNFs-C, represented by the red and blue lines). (B) Digital images of the PNFs films were captured before and after the addition of CA. (1) PNFs, (2) PNFs with 1 wt. % (PNFs-C1), and (3) 1.5 wt. % (PNFs-C1.5) of CA.

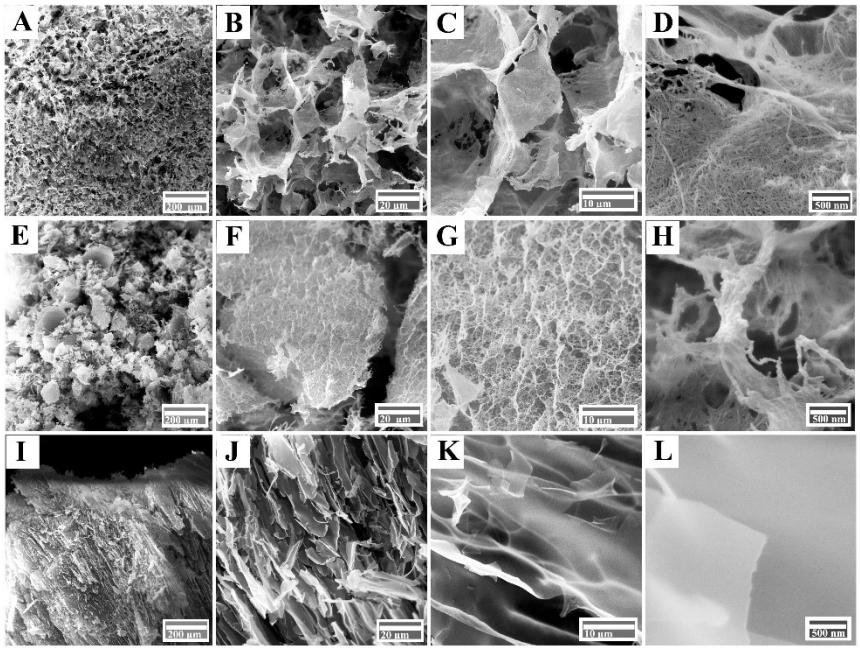

Fig. S2 Surface morphology of the freeze-dried biomaterials: FE-SEM images of (A) Cellulose nanofibers (CNFs) aerogel, (B-D) High-resolution images of CNFs aerogel illustrating the porous structure of the aerogel. E) Neat chitosan (Cs) aerogel, (F-H) High-resolution images of Cs aerogel demonstrating the integration of fibrils in the formation of the interconnected network. (I) PNFs aerogel, (J-L) High-resolution images of PNFs revealing compact layered sheets.

Table S1 Characteristics of Congo red (CR) [4]

CA Index name	1-Naphthalenesulfonic acid, 3,3'-[(1,1'-biphenyl)-4,4'-diylbis(2,1-diazenediyl)]bis[4-amino-,sodium salt (1:2)]
CAS No.	573-58-0
Molecular formula	$C_{32}H_{22}N_6Na_2O_6S_2$
Molecular weight	696.66 g mol^{-1}
Chemical Structure	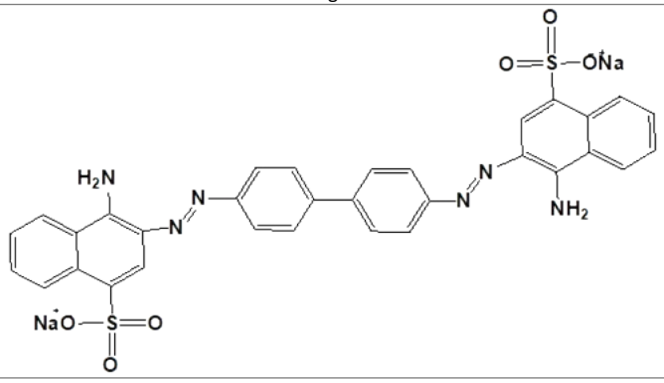
Molecular surface area	557.6 cm^2
Density	0.995 g cm^{-3} at 25 ºC

Electronic Supplementary Material (ESI) for Materials Advances.

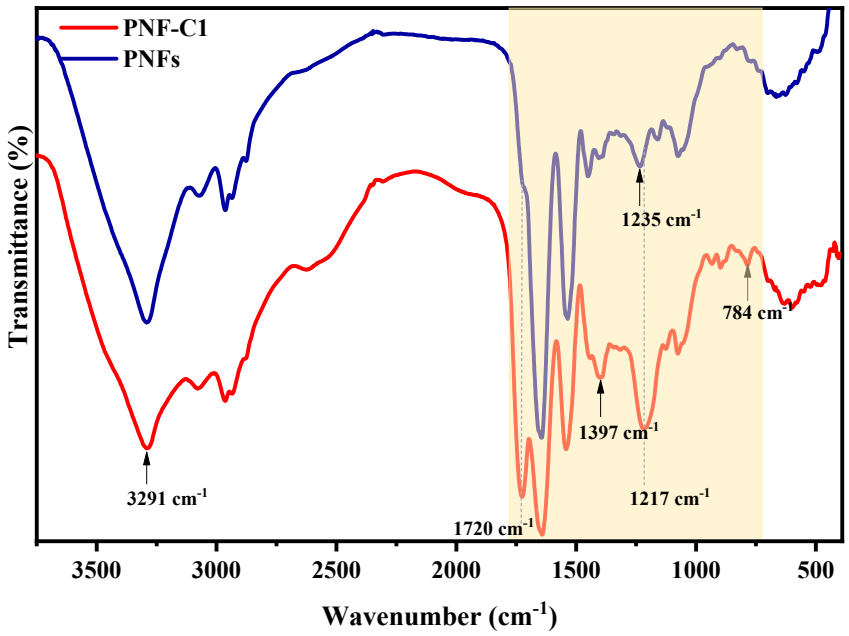

Fig. S3 FTIR spectra of PNFs before (PNFs, blue line) and after crosslinking with CA (PNF-C1, red line) shown in full range 3800-500 cm^{-1}.

Fig. S4 XRD spectra of CCs and CPCs composite aerogel beads and their counterparts (CNFs, Cs, and PNFs).

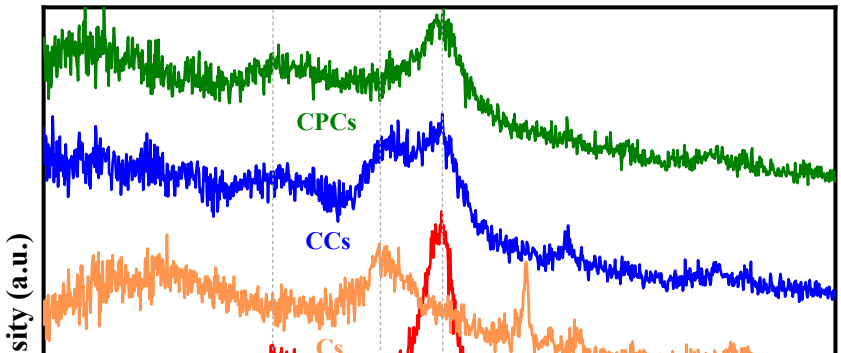

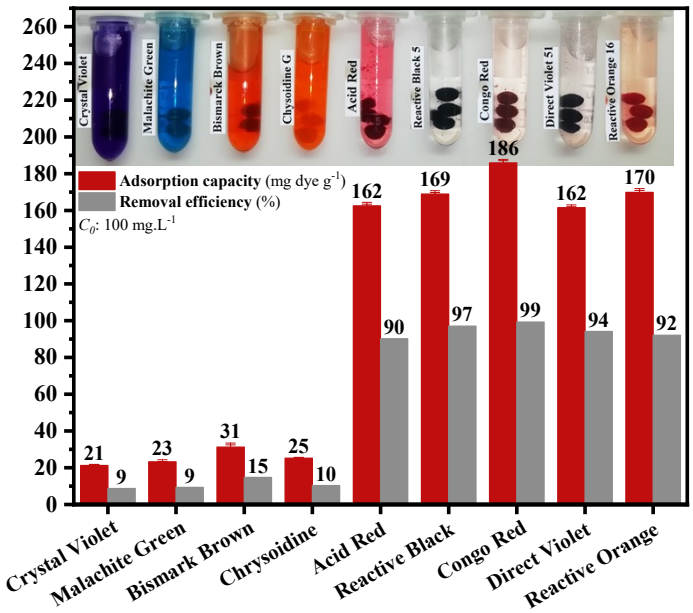

Fig. S5 The adsorption capacity and removal efficiency of CNFs/Cs/PNFs aerogel beads (CPCs) for removing various cationic and anionic dyes (The inset images representing remained dye solutions at adsorption equilibrium time).

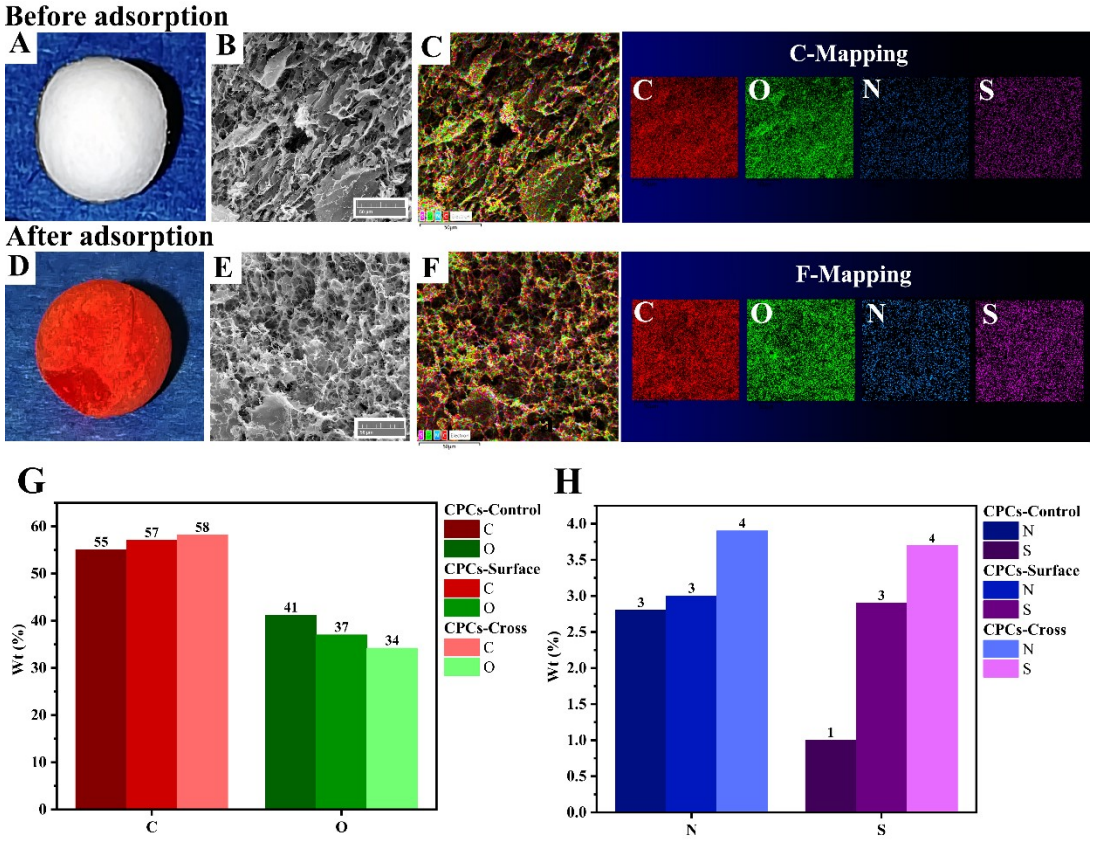

Fig. S6 Digital and FE-SEM images with corresponding EDX spectra and elemental mapping of C, O, N, and S for CPCs aerogel. (A-C) Before, and (D-F) After CR dye adsorption. Calculated values from the elemental maps of CPCs aerogel: (G) C and O, (H) N, and S.

Table S2 Comparison of maximum adsorption capacity of various polysaccharide and PNFs-based aerogels for CR.

Adsorbant	pH_{zpc}	Q_{max} (mg g^{-1})	Isotherm	Year	Ref.
Polysaccharide-based materials					
chitosan hydrobeads	6.4	93.71	Langmuir	2007	[5]
chitosan/montmorillonite	7	81.23	Langmuir	2007	[6]
chitosan/multiwalled carbon nanotubes	5	450.4	Langmuir	2010	[7]
cellulose/Fe_3O_4/activated carbon composites	natural pH	66.09	Langmuir	2011	[8]
cellulose/ chitosan hydrogel beads	7	40	Langmuir	2015	[9]
Tea waste	10	32.26	Langmuir	2015	[10]
Ni/Al mixed oxide microspheres	6	1229.59	SIP	2015	[11]
CaCO3-loaded cellulose aerogel	natural pH	75.81	-	2015	[12]
Chitosan Beads	6	166.67	Langmuir	2016	[13]
diammonium tartrate modified chitosan	8	1597	SIP	2017	[14]
Modified chitosan hydrogel beads	5	1994	SIP	2017	[15]
Cellulose/chitosan aerogel	7	381.7	Langmuir	2018	[16]
graphene–chitosan composite hydrogel	7	384.62	Langmuir	2018	[17]
dialdehyde micro fibrillated cellulose/ chitosan composite film	5.5	152.5	Langmuir	2018	[18]
chitosan-$Fe(OH)_3$ beads	8.39	445.32	Langmuir	2018	[19]
cellulose-chitosan foams	7.4	1170.2	Langmuir	2018	[20]
DAC-crosslinked cellulose-chitosan foam	7.4	1548.2	SIP	2019	[21]
Cationized rice husk cellulose	7.27	580.09	Langmuir	2019	[22]
pine bark	3.4	2.51	Freundlich	2019	[23]
graphene oxide/waste-newspaper cellulose aerogel	unadjusted pH	140.4	Langmuir	2020	[24]
Cellulose Nanofibril/Carbon Nanomaterial aerogel	natural pH	585.3	Langmuir	2020	[25]
chitosan/cellulose hydrogel	3	1480	Langmuir	2022	[26]
κ-carrageenan/polyacrylamide double network aerogel containing graphene oxide (GO)	7	20.718	Langmuir	2022	[27]
carboxyl cellulose nanofibers/montmorillonite/polyethyleneimine aerogel	unadjusted pH	3114	Langmuir	2022	[28]
waste bamboo paper and chitosan biohybrid aerogel	6.28	559.6	SIP	2022	[29]
magnetic hydroxyethyl cellulose/Fe_3O_4	7	308.64	Langmuir	2023	[30]
abundant sodium alginate (SA)/gellan gum aerogel	natural pH	576.5	Langmuir	2023	[31]
Extracted cellulose/chitosan aerogel	Origin pH	255.1	Langmuir	2023	[32]
Chitosan–Quinoa Bran Aerogel	5	182.48	Langmuir	2023	[33]
Chitosan/UiO-67 hydrogel	7.2	1001.2	Langmuir	2023	[34]
micro/nano MIL-88A (Fe, Al, Fe-Al)/ chitosan composite sponge	7.1-8.3	607-1312	SIP	2023	[35]
Protein nanofibrils and Protein Isolates					

powdered eggshell	8.8	95.25	Langmuir	2013	[36]
Industrial waste eggshell	7.09	49.5	Freundlich	2017	[37]
regenerated silk materials	not mentioned	above 96 percent rejection	not mentioned	2017	[38]
silk nanofibril (SNF)/ hydroxyapatite (HAP)		Flux rejection	not mentioned	2017	[39]
modified eggshell	4.5	117.65	Langmuir	2019	[40]
gluten materials	<6	211.1	Langmuir	2019	[41]
Protein Amyloid Fibrils aerogel	5.1	97.5	not mentioned	2022	[42]
Cellulose nanofibers/Chitosan/Protein nanofibrils aerogel beads	7.4	1349.8	SIP	2023	This work

References:

1 K. Gade Malmos, L. M. Blancas-Mejia, B. Weber, J. Buchner, M. Ramirez-Alvarado, H. Naiki and D. Otzen, *Amyloid Int. J. Exp. Clin. Investig. Off. J. Int. Soc. Amyloidosis*, 2017, **24**, 1–16.

2 B. Ma, X. You and F. Lu, *Int. J. Biol. Macromol.*, 2014, **64**, 162–167.

3 M. Peydayesh, M. Bagnani and R. Mezzenga, *ACS Sustain. Chem. Eng.*, 2021, **9**, 11916–11926.

4 S. Chatterjee, S. Chatterjee, B. P. Chatterjee and A. K. Guha, *Colloids Surfaces A Physicochem. Eng. Asp.*, 2007, **299**, 146–152.

5 S. Chatterjee, S. Chatterjee, B. P. Chatterjee and A. K. Guha, *Colloids Surfaces A Physicochem. Eng. Asp.*, 2007, **299**, 146–152.

6 L. Wang and A. Wang, *J. Hazard. Mater.*, 2007, **147**, 979–985.

7 S. Chatterjee, M. W. Lee and S. H. Woo, *Bioresour. Technol.*, 2010, **101**, 1800–1806.

8 H. Y. Zhu, Y. Q. Fu, R. Jiang, J. H. Jiang, L. Xiao, G. M. Zeng, S. L. Zhao and Y. Wang, *Chem. Eng. J.*, 2011, **173**, 494–502.

9 M. Li, Z. Wang and B. Li, *Desalin. Water Treat.*, 2016, **57**, 16970–16980.

10 M. Foroughi-Dahr, H. Abolghasemi, M. Esmaili, A. Shojamoradi and H. Fatoorehchi, *Chem. Eng. Commun.*, 2015, **202**, 181–193.

11 W. Huang, X. Yu and D. Li, *RSC Adv.*, 2015, **5**, 84937–84946.

12 K. Y. Chong, C. H. Chia, S. Zakaria, M. S. Sajab, S. W. Chook and P. S. Khiew, *Cellulose*, 2015, **22**, 2683–2691.

13 N. P. Raval, P. U. Shah, D. G. Ladha, P. M. Wadhwani and N. K. Shah, *Desalin. Water Treat.*, 2016, **57**, 9247–9262.

14 A. Zahir, Z. Aslam, M. S. Kamal, W. Ahmad, A. Abbas and R. A. Shawabkeh, *J. Mol. Liq.*, 2017, **244**, 211–218.

15 C. Lin, S. Li, M. Chen and R. Jiang, *J. Dispers. Sci. Technol.*, 2017, **38**, 46–57.

16 Y. Wang, H. Wang, H. Peng, Z. Wang, J. Wu and Z. Liu, *Fibers Polym.*, 2018, **19**, 340–349.

17 S. Omidi and A. Kakanejadifard, *RSC Adv.*, 2018, **8**, 12179–12189.

18 X. Zheng, X. Li, J. Li, L. Wang, W. Jin, Y. Pei and K. Tang, *Int. J. Biol. Macromol.*, 2018, **107**, 283–289.

19 XinxinYang, Y. Li, H. Gao, C. Wang, X. Zhang and H. Zhou, *Int. J. Biol. Macromol.*, 2018, **117**, 30–41.

20 U.-J. Kim, D. Kim, J. You, J. W. Choi, S. Kimura and M. Wada, *Cellulose*, 2018, **25**, 2615–2628.

21 U. J. Kim, S. Kimura and M. Wada, *Carbohydr. Polym.*, 2019, **214**, 294–302.

22 Z. Jiang and D. Hu, *J. Mol. Liq.*, 2019, **276**, 105–114.

23 K. Litefti, M. S. Freire, M. Stitou and J. González-Álvarez, *Sci. Rep.*, 2019, **9**, 1–11.

24 C. Feng, P. Ren, Z. Li, W. Tan, H. Zhang, Y. Jin and F. Ren, *New J. Chem.*, 2020, **44**, 2256–2267.

25 Z. Yu, C. Hu, A. B. Dichiara, W. Jiang and J. Gu, *Nanomaterials*, 2020, **10**, 1–20.

26 D. Li, J. Zhang, L. P. Li, G. Cai, W. Zuo, W. Zhan, P. Wang and Y. Tian, *J. Clean. Prod.*, 2022, **371**, 133650.

27 S. Tarashi, H. Nazockdast, S. Shafaghsorkh and G. Sodeifian, *Sep. Purif. Technol.*, 2022, **287**, 120587.

28 K. Fan, T. Zhang, S. Xiao, H. He, J. Yang and Z. Qin, *Int. J. Biol. Macromol.*, 2022, **211**, 1–14.

29 C. Qiu, Q. Tang, X. Zhang, M. C. Li, X. Zhang, J. Xie, S. Zhang, Z. Su, J. Qi, H. Xiao, Y. Chen, Y. Jiang, C. F. de Hoop and X. Huang, *J. Clean. Prod.*, 2022, **338**, 130550.

30 Y. Hui, R. Liu, L. Li, Q. Sun, Z. Xiao, A. Xu and S. Liu, *J. Porous Mater.*, 2023, **30**, 1735–1751.

31 Z. Qin, K. Dong, Y. Zhang, Y. Jiang, L. Mo and S. Xiao, *Bioresour. Technol.*, 2023, **370**, 128576.

32 Y. Liu, Y. Ke, Q. Shang, X. Yang, D. Wang and G. Liao, *Chem. Eng. J.*, 2023, **451**, 138934.

33 M. Tan, H. Lv, Q. Zhao, B. Wang, S. Zheng and K. Li, *Environ. Eng. Sci.*, 2023, **40**, 233–243.

34 Z. Jing, Y. Li, Y. Zhang, M. Wang, B. Chen, Y. Sun, K. Chen, Q. Du, X. Pi, Y. Wang, S. Zhao and Y. Jin, *ChemistrySelect*, 2023, **8**, 202204367.

35 Y. Jin, Y. Li, Q. Du, B. Chen, K. Chen, Y. Zhang, M. Wang, Y. Sun, S. Zhao, Z. Jing, J. Wang, X. Pi and Y. Q. Wang, *Microporous Mesoporous Mater.*, 2023, **348**, 112404.

36 M. A. Zulfikar and H. Setiyanto, *Int. J. ChemTech Res.*, 2013, **5**, 1532–1540.

37 M. A. Abdel-Khalek, M. K. Abdel Rahman and A. A. Francis, *J. Environ. Chem. Eng.*, 2017, **5**, 319–327.

38 L. Lv, X. Han, L. Zong, M. Li, J. You, X. Wu and C. Li, *ACS Nano*, 2017, **11**, 8178–8184.

39 S. Ling, Z. Qin, W. Huang, S. Cao, D. L. Kaplan and M. J. Buehler, *Sci. Adv.*, 2017, **3**, 1–12.

40 S. Parvin, B. K. Biswas, M. A. Rahman, M. H. Rahman, M. S. Anik and M. R. Uddin, *Chemosphere*, 2019, **236**, 124326.

41 X. Zhang, Y. Li, M. Li, H. Zheng, Q. Du, H. Li, Y. Wang, D. Wang, C. Wang, K. Sui, H. Li and Y. Xia, *J. Colloid Interface Sci.*, 2019, **556**, 249–257.

42 X. Jia, M. Peydayesh, Q. Huang and R. Mezzenga, *Small*, 2022, **18**, 2105502.